



Experimental investigation of the stochastic early flame propagation after ignition by a low-energy electrical discharge



Stefan Essmann^{a,*}, Detlev Markus^a, Holger Grosshans^a, Ulrich Maas^b

^aPhysikalisch-Technische Bundesanstalt (PTB), Bundesallee 100, Braunschweig 38116, Germany

^bInstitute of Technical Thermodynamics, Karlsruhe Institute of Technology, Engelbert-Arnold-Str. 4, Karlsruhe 76131, Germany

ARTICLE INFO

Article history:

Received 1 March 2019

Revised 11 April 2019

Accepted 15 September 2019

Keywords:

Spark ignition
Minimum ignition energy
Lewis number
High-speed schlieren

ABSTRACT

In the context of explosion protection, very conservative safety factors need to be considered, e.g. in the design of electrical devices. This is due to standards which are mainly based on empirical data as opposed to a detailed knowledge of the underlying physiochemical processes. In this work, the early phase of ignition of burnable gas mixtures close to their respective minimum ignition energy is investigated experimentally by means of high-speed schlieren imaging. Our data quantifies how the ignition process at such low energies becomes less repeatable which is evidenced by a high scattering of the flame propagation. It was found that, depending on the mixture, the flow field induced by the electrical discharge may exhibit a considerable effect on the ignition process. This effect is more pronounced for mixtures which are characterized by a large Lewis number, thus, leading to a more random flame propagation.

© 2019 The Author(s). Published by Elsevier Inc. on behalf of The Combustion Institute. This is an open access article under the CC BY-NC-ND license. (<http://creativecommons.org/licenses/by-nc-nd/4.0/>)

1. Introduction

In safety engineering and the process industry, electrostatic discharges pose a potential risk as ignition sources which must be avoided. An important safety characteristic property of burnable gases which is used in this context is the minimum ignition energy (MIE). A specific obstacle in the prevention of fatal explosions in industrial facilities lies in the highly random behavior of ignitions at energy levels close to MIE. In the frame of forced ignition, such as in automotive engines, the MIE is often defined as the energy where a given mixture ignites 50% of the time [1–3]. However, regarding safety-relevant ignition processes a 50% chance of ignition is too high to be tolerated. Therefore, in this context the MIE is defined as the energy where one in 100 electrical discharges ignites the most ignitable mixture of a burnable gas with air or another oxidizer [4,5]. Due to their perceived randomness, the characteristics of ignitions near the MIE are quantitatively and qualitatively substantially different from the commonly investigated case of high energy input, such as automotive spark ignition. A detailed discussion of the ignition probability of the MIE can be found in the appendix of [6].

At discharge energies close to the MIE of typical combustibles like hydrogen, ethene, and propane (which all have MIEs considerably smaller than 1 mJ), loss processes play an important role for the ignition and transition to a self-sustained flame propagation. They include external (ohmic) losses in the electric circuit, heat transfer to the electrodes, radiation, and losses due to the development of a shock wave [7]. In addition, the MIE depends not only on the substance under investigation but also on the method used to determine it, specifically the electrode geometry and arrangement as well as discharge characteristics [8–10].

Near the MIE, ignition has a stochastic nature so that there is only a limited probability of ignition. This was pointed out by Bane et al. [11] who investigated the statistical nature of spark ignition and the role of the MIE for a range of combustibles with relevance to aviation safety [6,11,12]. In particular, the MIE is not a threshold value that segregates a non-ignition regime from an ignition regime. A logistic fit of the ignition probability was proposed which allows for a more accurate assessment of the risk of explosions than the MIE alone. Thereupon, other researchers have used this method to determine the properties of other combustibles. Eckhoff et al. [13] found that for propane the probability of ignition at the MIE is below 1%. The measurements by Wähler et al. [14] showed that the probability of ignition at the MIE is between 0.1% and 1% for hydrogen, ethene, and propane.

The effect of ignition energy on the ignition of propane/air mixtures was investigated by Lim et al. [15]. They identified the causes

* Corresponding author.

E-mail address: stefan.essmann@ptb.de (S. Essmann).

of early and later kernel growth to be mass entrainment and diffusion, respectively. The boundary conditions of this work were, however, not close to MIE conditions relevant for explosion protection applications. Champion et al. [16] compared a numerical model for spherical flame initiation to experimental results. They proposed the existence of a critical spherical flame radius for successful ignition of lean mixtures of heavy fuels. Research focused on the flame kernel formation induced by short-duration sparks was performed by Kono et al. [17]. The calculations were performed for nitrogen and were able to describe the kernel shape in good agreement with the ones observed in experiments with propane/air mixtures. This demonstrated that the gas flow pattern is the main cause for the kernel configuration. Borghese et al. [18] investigated the ignition of propane/air at elevated pressure and described in detail several phases of the early flame propagation: the fast expansion of the spark channel, the build-up and detachment of a shock wave and the development of a flow field which influences the further flame propagation. The relative importance of the flow field and chemistry were analyzed. Nevertheless, this work was related to forced ignition at elevated pressure and limited to propane. Near-MIE conditions of propane/air were investigated by Ko et al. [19] with the laser-schlieren technique. The different phases of early flame propagation were described and loss processes were identified via spark calorimetry. In this study, the 50% definition of MIE was used; hence, the ignition energies tested were around one order of magnitude larger than the MIE defined at 1% ignition probability. Pitt et al. [20] studied in detail the toroidal flow structure and the mixing connected with it. The transition from laminar to turbulent mixing was taken into account in their study. However, the ignition energies considered were 162 mJ – much larger than the MIEs of the gases considered in our work. For methane/air mixtures, the effects of discharge energy and loss processes were analyzed thoroughly [21], but no extension to other fuels was carried out in this study.

As regards the ignition of hydrogen/air mixtures, numerical studies [22,23] as well as detailed experimental works have been performed. Ono and Oda [24] looked into ignitions at energies close to the MIE using laser-induced pre-dissociation fluorescence for a stoichiometric and a rich mixture. The effect of ignition energy was discussed and the different regimes of flame propagation were identified. However, the stochastic nature of ignition at such low ignition energies was not considered in their work. Further, the critical radius for ignition, its relationship to the ignition energy and the dependence on the Lewis number of the combustible mixture were investigated by Chen et al. [25,26] and Zhou et al. [27]. Although the different flame trajectories for varying initial conditions were discussed, the stochastic variability at energies close to the MIE was not analyzed.

The flow field which is induced by electrical discharges in a two-electrode arrangement was described by Kono et al. [1,28] for two successive sparks in propane/air mixtures. Bane et al. [29] studied the effect of different electrode geometries on the resulting flow pattern in spark ignition situations relevant for industrial and aviation safety by means of numerical simulations and schlieren experiments. The study was limited to ignitions in hydrogen/air mixtures but clearly showed the importance of the electrode shape on the ignition process. The varied geometry of the electrodes (cylindrical, conical and flanged) induced different flow fields which strongly influenced the ignition. Recently, Singh et al. [30] studied the flow field induced by the discharge using particle image velocimetry.

Despite all these research efforts, even after decades of research starting with the works of Lewis and von Elbe [4], the prediction of safety-relevant ignition processes is not feasible with the current numerical models. This is due to a lack of knowledge concerning the physical and chemical processes leading to the ignition

by low-energy electrical discharges relevant to explosion safety. Hence, standards for the design and testing of explosion protected devices are mainly based on empirical data [5,10,31,32]. Consequently, relatively large safety factors need to be considered, for example, in the development of explosion protected devices and the control of processes in the chemical and petrochemical industry. Thus, a more detailed knowledge of the physical and chemical processes underlying the ignition by electrical discharges at near-MIE conditions could help to improve those standards. Subsequently, it could lead to economic benefits for producers of explosion protected equipment as well as operators of processes where explosion risks need to be considered.

This study aims to contribute to closing this gap. We investigate the ignition of the most ignitable hydrogen/air, ethene/air, and propane/air mixtures by electrical discharges close to the respective MIE experimentally. High-speed schlieren imaging of the early expansion of the flame kernel is employed to study single ignition processes. We analyze the stochastic behavior of the ignition and the early flame propagation. Furthermore, we discuss the effects of ignition energy, the flow field, Lewis number, and flame stretch on the early flame propagation. The findings from this study can be used to improve numerical models to predict safety-relevant ignition processes.

2. Experiment

2.1. Discharge circuit and initiation of discharges

Electrical discharges were generated between two tungsten rod electrodes (2.4 mm diameter) with rounded tips (hemisphere electrode arrangement) which were placed inside an optically accessible stainless steel test vessel. Previous experiments showed that the use of such electrodes allowed ignition of the investigated mixtures at their respective MIE [14,33]. The vessel was flushed with burnable gas/air mixture until its volume had been exchanged at least five times. The mixtures were produced via mass flow controllers (Bronkhorst EL-FLOW) and controlled through their oxygen content which was measured with an oxygen analyzer (Servomex MiniHD 5200). Three mixtures were investigated at conditions close to the respective MIE (Table 1). These MIE conditions comprise the optimal mixture composition and the optimal electrode distance where optimal in this context means that the ignition energy is minimized. The most ignitable mixture composition and corresponding electrode distance were chosen according to Wöhner et al. [14]. At larger or smaller electrode distances, the required ignition energy increases. Thus, to be able to perform experiments at energies as close to the MIE as possible, the electrode distances are different for each mixture and are kept constant throughout the experiments. The effective Lewis numbers given in Table 1 were calculated via the approach by Addabbo et al. [34] using *Cantera* [35] and thermodynamic data from GRI 3.0 [36]. Table 1 also lists the mixture-averaged diffusion coefficients used in the calculations.

The electrical circuit (Fig. 1) consisted of the electrodes, a high-voltage source, a variable capacitor in parallel to the spark gap, and a large resistor in between the source and the spark gap to prevent continuous discharges. A high-voltage probe was attached to the top electrode for measuring the voltage at breakdown. In addition, a current transformer picked up the discharge current. The discharge energy could be adjusted by the variable capacitor via the relation $E = 1/2 CU^2$, where E is the discharge energy, C is the capacitance of the set-up, and U is the voltage at breakdown. Further details concerning the discharges and the set-up may be found in [37]. The discharges were precisely triggered by means of ultraviolet radiation from an Nd:YAG laser [38]. The experiments were carried out at room temperature ($21.5 \pm 1.0^\circ\text{C}$) and

Table 1
MIE conditions of the burnable gases investigated. v – concentration in air, φ – equivalence ratio, MIE – minimum ignition energy, d – electrode distance, Le – effective Lewis number of the mixture, $\mathcal{D}_{\text{fuel}}$ – mixture-averaged diffusion coefficient of the fuel, \mathcal{D}_{O_2} – mixture-averaged diffusion coefficient of O_2 .

Burnable gas	v [14]	φ	MIE [5]	d [14]	Le	$\mathcal{D}_{\text{fuel}}$	\mathcal{D}_{O_2}
Hydrogen	23.3 vol%	0.72	17 μJ	0.5 mm	0.56	$1.001 \times 10^{-4} \text{ m}^2/\text{s}$	$2.415 \times 10^{-5} \text{ m}^2/\text{s}$
Ethene	8.0 vol%	1.24	82 μJ	1.2 mm	1.11	$1.609 \times 10^{-5} \text{ m}^2/\text{s}$	$1.970 \times 10^{-5} \text{ m}^2/\text{s}$
Propane	5.2 vol%	1.31	240 μJ	1.7 mm	1.17	$1.108 \times 10^{-5} \text{ m}^2/\text{s}$	$1.936 \times 10^{-5} \text{ m}^2/\text{s}$

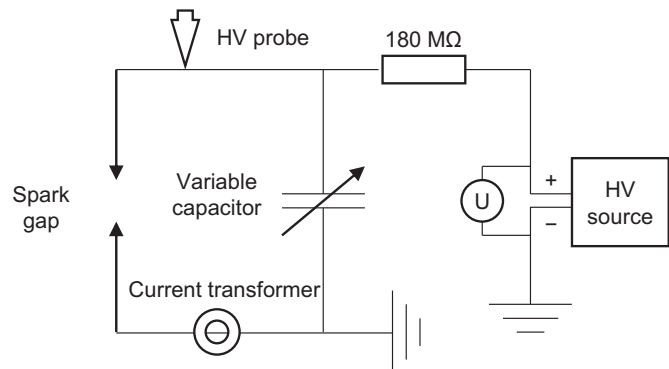


Fig. 1. Sketch of the electrical set-up for the generation of low-energy discharges.

atmospheric pressure ($1000 \pm 40 \text{ mbar}$). After each ignition, the vessel was flushed with dried air sufficiently long until no reaction products remained and the vessel temperature was at room temperature. In order to examine stochastic fluctuations in the ignition process, the experiment was repeated for each energy level until at least five ignitions were observed or, for cases with very low ignition probability, up to a maximum of 100 trials (with or without ignition).

The ignition process was investigated at four energy levels close to the respective MIE of each mixture (Table 2). For hydrogen the lowest energy we were able to investigate with our set-up was 2.3 MIE due to internal capacitances of the set-up. Since the voltage needs to be in a certain interval for each configuration, the minimum energy is determined by the capacitance. The ignition probabilities P_{ign} for each configuration given in Table 2 were calculated based on the logistic regression formulas given in [14], which in turn are based on the large number of experiments reported in that work.

Table 2
Ignition probabilities for the energy levels investigated, rounded to three significant digits [14].

Hydrogen		Ethene		Propane	
E/MIE	P_{ign} (%)	E/MIE	P_{ign} (%)	E/MIE	P_{ign} (%)
2.3	99.0	1.5	6.80	1.5	0.28
3.4	100	2.0	41.0	2.0	1.08
4.5	100	2.9	97.6	2.9	12.1
5.6	100	3.8	100	4.0	75.4

2.2. High-speed schlieren imaging

We investigated the early phase of flame propagation with the schlieren technique [39]. A high-power LED (Luminus SBT-70-G) in continuous wave mode in combination with a pinhole was used as a light source. The set-up consisted of two 500 mm field lenses and another pinhole as the schlieren stop. A high-speed camera (Photron Fastcam SA-5) was used to record schlieren images at 62.5 kHz. The images were post-processed in Matlab in order to find the kernel radius in each frame. Details are found in the supplementary material.

3. Results and discussion

3.1. Early flame propagation

We recorded high-speed schlieren videos of the early phase following an electrical discharge in a burnable gas mixture to investigate the reasons for the stochastic behavior of the ignition. Figures 2–4 display selected series of such schlieren images. For each investigated gas mixture, different levels of ignition energy are compared. In the case of hydrogen (Fig. 2), only a minuscule variation between the discharge energies is visible. Hence, only two energies are shown in this figure. An increase in ignition en-

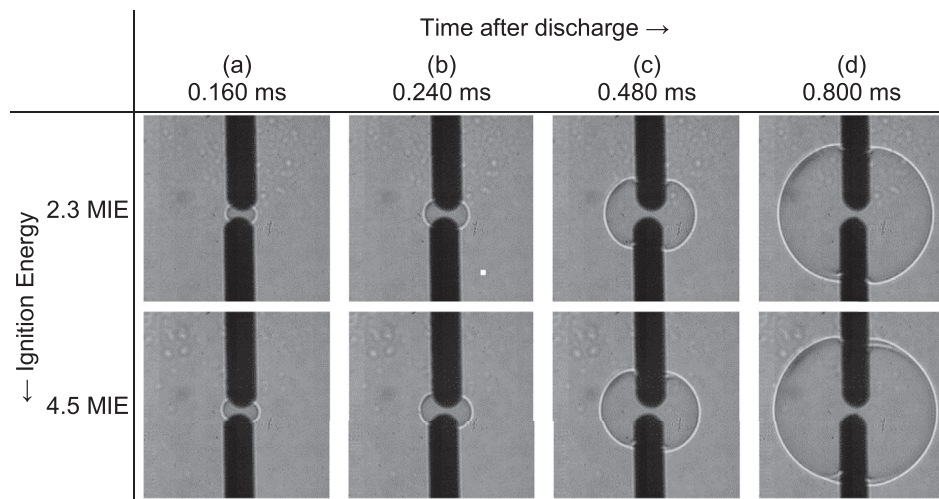


Fig. 2. Series of schlieren images showing the early phase of flame kernel expansion after ignition by an electrical discharge in a 23.3 vol% hydrogen/air mixture (0.5 mm electrode distance). Each row corresponds to a specific ignition energy indicated on the left while the columns are labeled with the time after ignition. The images were enhanced in brightness and contrast for better visualization.

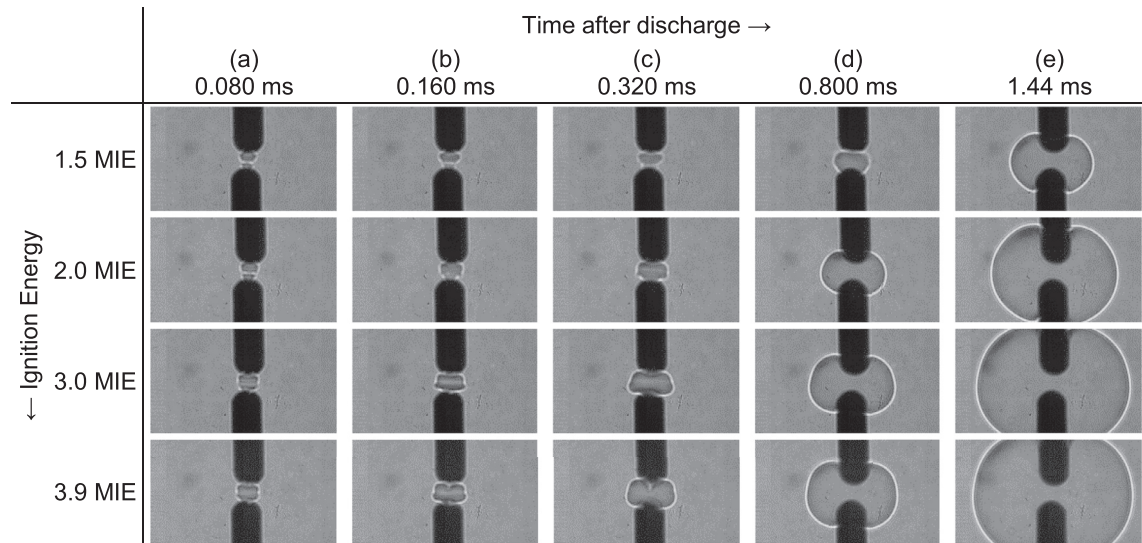


Fig. 3. Series of schlieren images showing the early phase of flame kernel expansion after ignition by an electrical discharge in an 8.0 vol% ethene/air mixture (1.2 mm electrode distance).

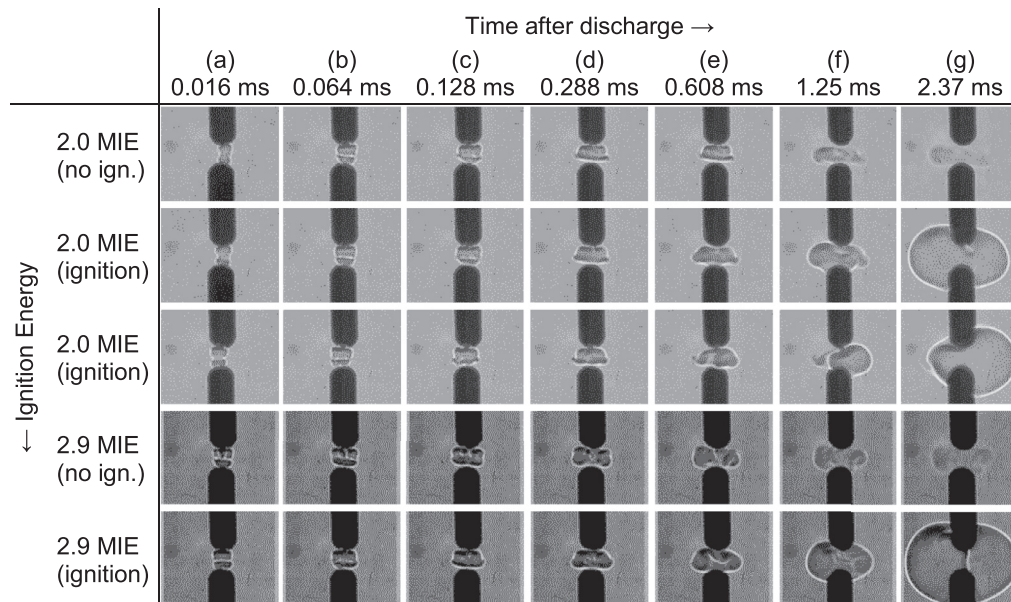


Fig. 4. Series of schlieren images showing the early phase of flame kernel expansion after ignition by an electrical discharge in a 5.2 vol% propane/air mixture (1.7 mm electrode distance).

ergy leads to a slightly larger flame for the same time after ignition. Of course, the ignition probability was very high in all cases that we were able to investigate (cf. Table 2). The flame appears to be spherical from the start.

For ethene (Fig. 3), larger differences can be observed. When the energy is increased the early flame growth becomes faster. The shape of the flame kernel in frames (a) and (b) is asymmetrical in axial direction at low energies and becomes more uniform at larger energies. At low energies the ignition process is very sensitive to changes in ignition energy. This could be explained by the fact that the ignition delay time is a non-linear function of the discharge energy. Therefore, at low energies the time scale at which processes may interfere with the ignition is much longer than at larger energies. On the other hand, at sufficiently large ignition energies, bigger absolute changes in the ignition energy are required for a significant change in the early flame kernel propagation. Thus, the flame kernels at 3.0 MIE and 3.9 MIE are very similar.

Even larger variations of the ignition process are observed in the propane mixture (Fig. 4). Here, we compare ignition events

and non-ignition events at two energy levels. Up to frame (d) (0.288 ms), the kernel expansion is very similar for ignitions and non-ignitions at the same energy. After 0.6 ms (frame (e)), small differences become visible. The kernel in the ignition case has expanded a little further than the non-igniting kernel. The frames (f) and (g) (1.25 ms and 2.37 ms) illustrate how the non-igniting kernel cools down while the flame propagates in the other case. As the image series of ignitions at 2.0 MIE (rows two and three) demonstrate, there is substantial variation between igniting cases at low ignition energy. For reference, the ignition probability for propane/air at 2.0 MIE is only around 1% (cf. Table 2). In the ignition case in the third row, the discharge occurs not in the center between the electrodes but offset to the left-hand side. Therefore, the vortices which are induced in the flow field due to the discharge and the fast expansion of the kernel [28,29,40,41] should be asymmetrical. It appears that the kernel is convectively transported to the right-hand side where, eventually, the ignition occurs. Such one-sided ignition events were observed only in the propane/air mixture and only at 2.0 MIE and 2.9 MIE. They have in

common that the position of the discharge was slightly off-center, i.e., shifted from the electrode axis by up to one quarter of the electrode diameter (0.6 mm). This can happen due to microscopic changes of the electrode surface induced by previous discharges which locally change the electric field and thereby the most likely location of the discharge. This effect would not be expected with pointed electrodes. However, pointed electrodes would change the characteristics of the flow field [29]. In general, the ignition process becomes more reproducible with increasing ignition energy and the flame becomes more symmetrical. At 4.0 MIE, we did not observe single-side ignition events even when the discharge was off-center.

The kernel radii that were extracted from the schlieren images for different ignition energies are compared in Fig. 5. Only successful ignition events are shown here. Individual experiments are represented by dashed lines while solid lines indicate the average values for each energy level. In addition to the reduced ignition probability, this data ascertains the enhanced fluctuation of the flame propagation at low energies.

The hydrogen kernels (Fig. 5(a)) closely follow a single line at constant ignition energy. When the energy is increased, the kernel expansion is enhanced during the period up to 0.1 ms after ignition and the ignition delay time appears to decrease slightly. After this time, the ignition source has no further effect on the kernel propagation. Bradley and Lung [42] called this the *spark assisted flame propagation regime*. Its duration depends on the combustible gas/air mixture and the ignition energy. Overall, the effect of ignition energy is small for the energy range investigated for hydrogen. Between the highest two energy levels (4.5 MIE and 5.6 MIE), no significant change in the kernel propagation can be observed.

In the case of ethene (Fig. 5(b)), substantial variation is present at low ignition energies. At 1.5 MIE and 2.0 MIE, there is considerable scatter between individual experiments. The scatter becomes smaller for the larger energies investigated. Moreover, all curves approach the same slope after about 1 ms when only chemistry and stretch due to the spherical flame shape govern the flame propagation. However, during the first 0.5 ms, the ignition source still plays an important role. For the kernels of low ignition energy, the spark assistance is relatively weak. Thus, they propagate very slowly up to 0.5 ms. Then, they accelerate until the average kernel propagation speed reaches a constant value. This effect is due to the fact that the Lewis number of the ethene/air mixture is significantly larger than unity. Therefore, positive stretch as it occurs especially in spherically expanding flames of small diameter impedes the flame front propagation. As the flame kernel grows, the stretch reduces and thus, the kernel propagation speed increases. The Lewis number effect will be further discussed in Section 3.3. At larger ignition energies, the flames start with a speed that is even higher, approaching the same average kernel propagation speed from above. This is due to the aforementioned spark assisted flame propagation. There is a clear effect of an increase in ignition energy on the ignition process and early kernel propagation such that ignition becomes faster and more reliable.

Figure 5(c) compares the early kernel propagation in the propane/air mixture for varying ignition energy. No ignitions were observed in 100 trials at an energy level of 1.5 MIE. An increase in ignition energy yields more reproducible results. The one-sided ignition events (dotted lines) occur quite often at 2.0 MIE and 2.9 MIE but not at 4.0 MIE. There is no observable shift towards faster or slower kernel growth compared to the normal ignition events at the same energy. For this mixture, the effect of the ignition source is evident for about 0.5 ms.

The results illustrate the stochastic behavior of the ignition process in burnable gas/air mixtures at energies close to the respective MIE. In practice, small deviations from the nominal mixture composition, fluctuations in the initial temperature and initial pressure,

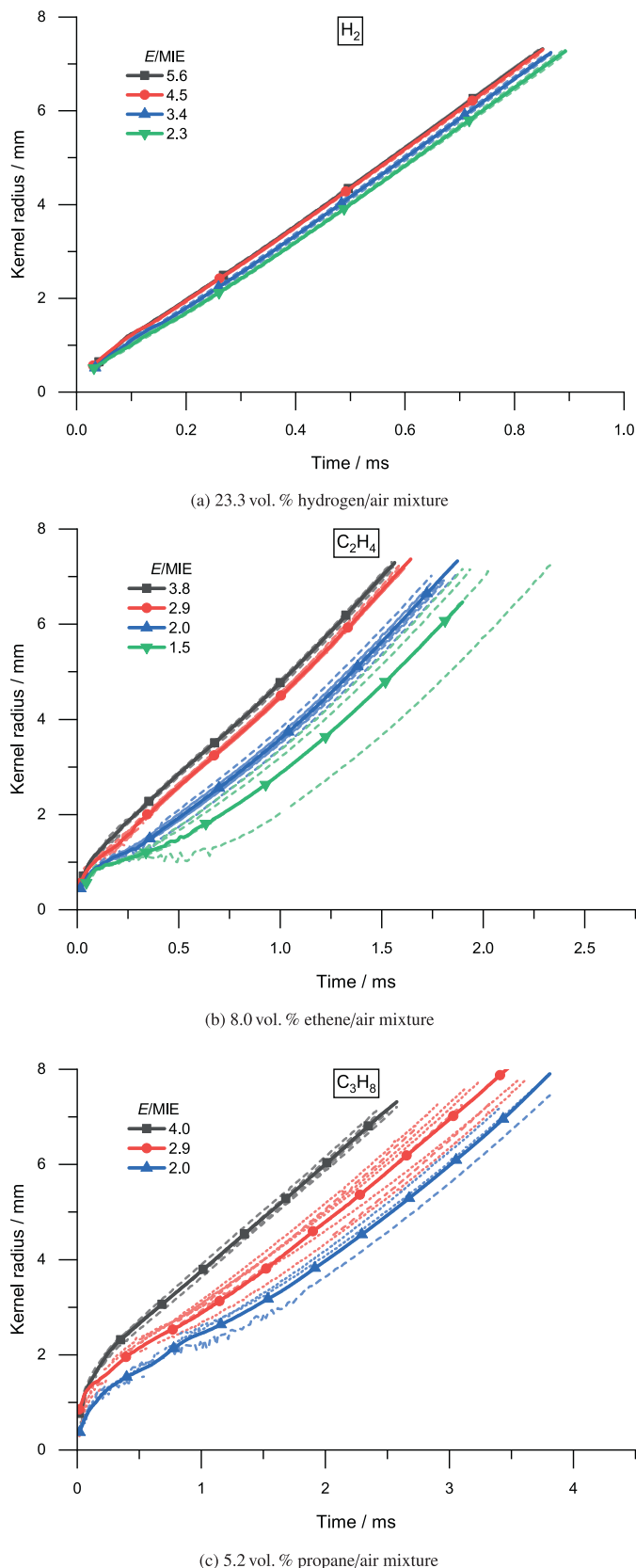


Fig. 5. Kernel radius as a function of time after discharge for several ignition energies close to the minimum ignition energy, extracted from the schlieren images. The dashed lines indicate individual experiments; solid, bold lines indicate the respective average values. The dotted lines in (c) correspond to experiments where a one-sided ignition was observed.

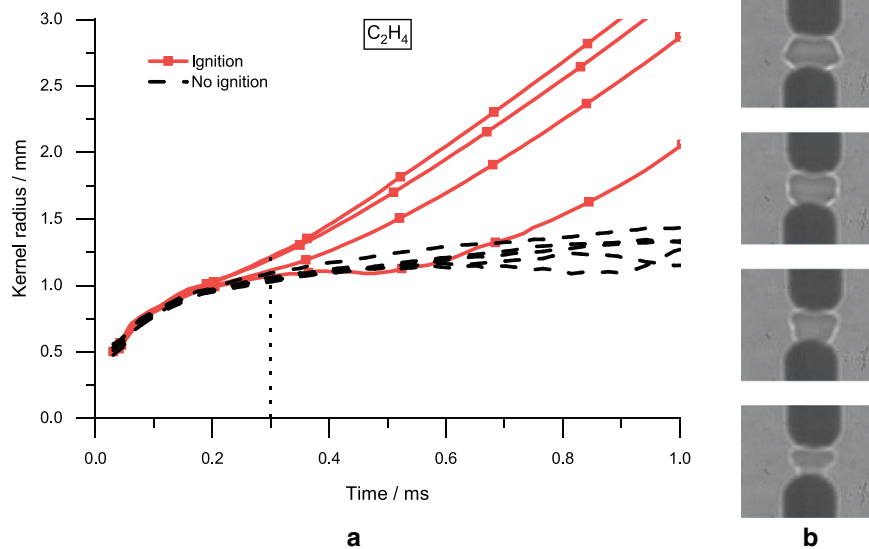


Fig. 6. Ignition and non-ignition events in an 8.0 vol% ethene/air mixture at $E = 1.5\text{MIE}$ ($P_{\text{ign}} = 6.8\%$). (a) Kernel radius as a function of time, (b) schlieren images of the flame kernels of the four ignition events at 0.3 ms (as indicated by the dotted line in the diagram). The order of the images (top to bottom) corresponds to the order of the four solid curves in (a).

and non-quiet fluid in the vessel are always present. If the discharge energy is sufficiently large, these small deviations do not affect the ignition process. At energies very close to the MIE, however, the ignition process is very sensitive to disturbances which is manifested in the scatter in the plots of the propane and ethene cases.

The observations from our experiments match the ignition probabilities given in Table 2: high ignition probabilities correspond to small deviations while low ignition probabilities correspond to a large scatter between repeated experiments. For instance, all investigated hydrogen cases have an ignition probability of 99% to 100%. Consequently, the ignition process is very stable and we did not observe any non-ignitions for these energies. In the case of ethene, the lowest energy tested (1.5 MIE) only has a 6.8% chance of ignition and, correspondingly, a large variation in the development of the igniting kernels can be observed.

This becomes very clear in Fig. 6 where the traces of four ignitions and five non-ignition events in the 8.0 vol% ethene/air mixture are compared. All curves closely follow a common trajectory up to 0.2 ms, where the kernel radius is close to 1 mm. Then, ignition events are observed in the time interval from 0.2 ms and 0.6 ms. From this long duration one can conclude that here processes that facilitate the continuation of the combustion process on one hand, and loss processes on the other hand which quench chemical reactions, occur on the same order of magnitude. The main factor influencing the chemical rate is the temperature, as is evident in Arrhenius equations describing the rate constants [43]. Here, the temperature field induced by the electrical discharge reaches values where the rate constants for the dominating reactions lead to conversion of chemical energy to heat which is counteracted by loss processes at a similar rate. These loss processes include cooling due to mixing with cold gas, heat conduction to the electrodes and radical quenching at the metal electrode surface.

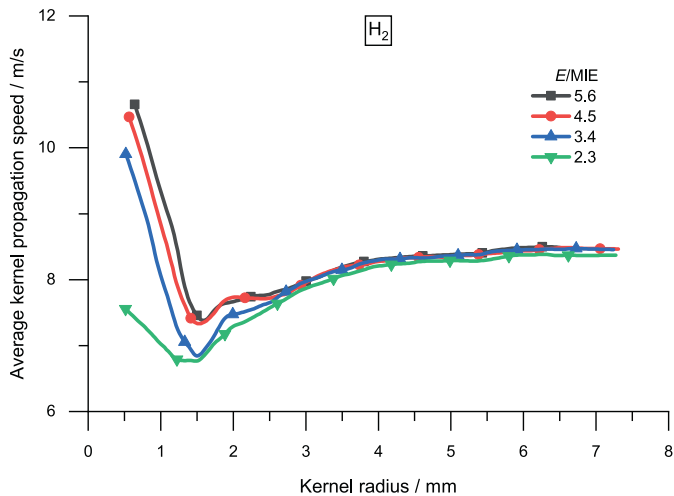
At the next energy level (2.0 MIE), the ignition probability is already 41% and indeed we observe less scatter between repeated experiments and thus better reproducibility of the ignition event. We can conclude that the elevated temperature field induced by a 2.0 MIE discharge compared to that of a 1.5 MIE discharge increases the reaction rates considerably. Therefore, relatively small perturbations through the aforementioned loss processes do not lead to quenching of the flame. Statistically, however, also larger

perturbations may occur, albeit less often. These will still lead to “non-ignition” events which is manifested in the observed ignition probability. For the higher energies, the ignition probability is close to 100%, yielding almost no variation in the different experiments. Still, the higher ignition energy affects the early flame kernel expansion.

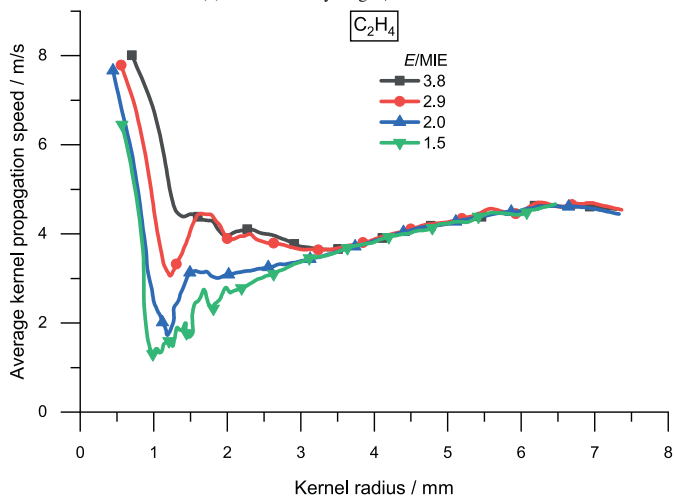
For propane, the distribution of the ignition probability is more spread out than that of ethene (cf. Table 2). Therefore, the variations in the experiments are larger even at higher E/MIE values: there is considerable scatter present in the kernel trajectories at 2.9 MIE (cf. Fig. 5(c)). Only at 4.0 MIE ignition energy, where the ignition probability is about 75%, the ignition process becomes more reliable.

Figure 7 shows the average kernel propagation speed obtained from the averaged flame trajectories in Fig. 5 as a function of the kernel radius. The average kernel propagation speed was calculated as dR_f/dt , where R_f is the flame kernel radius. For all mixtures, three regimes of the early flame propagation can be identified. First, the kernel expansion is over-driven due to the energy input from the electrical discharge. Here, the average kernel propagation speed is greater when the ignition energy is large. Second, a transition phase occurs, during which the average kernel propagation speed reaches a minimum value for the case of successful ignition. In cases where no ignition occurs (not shown here), the kernel trajectory follows the same path in this plot but would keep falling towards zero from this point on. The radius at which the minimum average kernel propagation speed is reached can be thought of as having a similar meaning as the critical spherical radius identified by Champion et al. [16] and the critical ignition volume postulated by Bradley and Lung [42]. In case of ignition, the average kernel propagation speed finally approaches a value that is independent of the ignition energy. This is when the third regime of early flame propagation is reached.

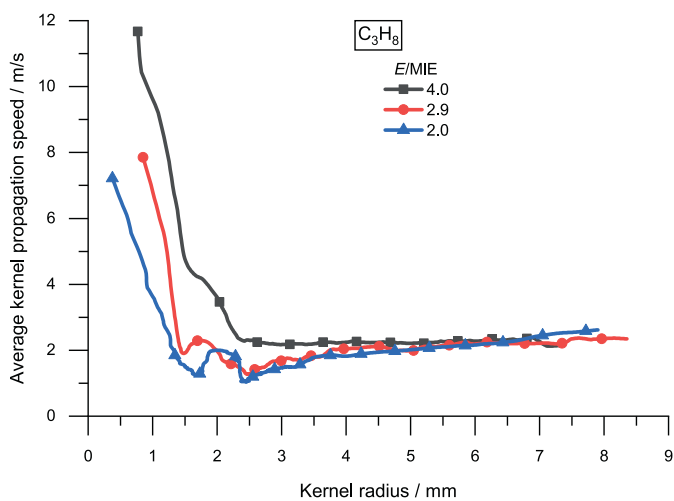
As Fig. 7 demonstrates, there exists a mixture-dependent radius where the transition phase is completed and the flames reach a common propagation speed. This radius is smallest for hydrogen (about 3 mm), followed by ethene (about 3.5 mm and 4 mm) and largest for propane (> 5 mm). Thus, an effect of the dissimilar Lewis numbers of the mixtures can be observed here. It is discussed further in Section 3.3. Another interesting point to note is that the minimum of the average kernel propagation speed is not



(a) 23.3 vol. % hydrogen/air mixture



(b) 8.0 vol. % ethene/air mixture



(c) 5.2 vol. % propane/air mixture

Fig. 7. Average kernel propagation speed over kernel radius for several ignition energies close to the minimum ignition energy. The jagged behavior of some curves is due to the stochastic fluctuations of the early flame propagation.

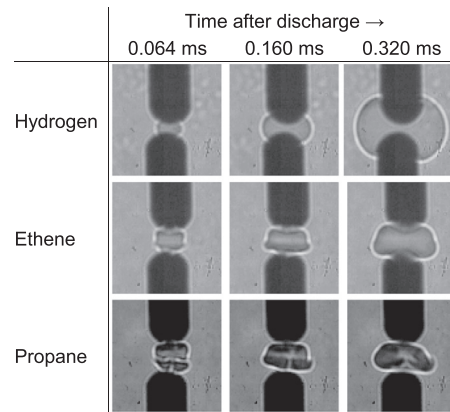


Fig. 8. Structure of early flame kernels for the most ignitable mixtures of hydrogen, ethene, and propane with air at $E \approx 3MIE$, shown for three time steps.

as pronounced for propane (Fig. 7(c)) as it is for the other mixtures. Again, this is a manifestation of the necessity for the spark assisted flame propagation for mixtures with $Le > 1$ [42].

3.2. Flame kernel structure

In an attempt to determine the reasons for the stochastic behavior of the ignition and the scatter in flame front propagation, we analyze the flame kernel structure for each mixture. Figure 8 compares the structure of the early flame kernels for the three mixtures. A representative ignition was chosen for each mixture. The hydrogen kernel is close to a spherical shape and not corrugated. The propane kernel is corrugated and stretched out in the direction perpendicular to the electrode axis. The ethene kernel is not spherical in shape and corrugated, but not as corrugated as the propane kernel.

One reason for the differences in the kernel structure in the first frame shown (0.064 ms) are the dissimilar ignition energies. While E/MIE is approximately constant for the kernels in Fig. 8, the absolute energies differ by an order of magnitude (51 μJ , 246 μJ and 720 μJ for hydrogen, ethene, and propane, respectively). Thus, the expansion of the hot gas channel, the induced pressure wave, and the vortex structure formed due to the presence of the electrodes are stronger at a higher absolute discharge energy [37,40]. Further, the electrode distance and shape influence the flow field which is induced by the discharge. The flow velocity increases as the spark gap increases [30,44]. Hence, both the larger electrode distance and the higher discharge energy lead to a higher flow velocity in the propane case compared to the ethene and the hydrogen case (the electrode distances are 1.7 mm, 1.2 mm and 0.5 mm, respectively). In addition to these gas-dynamic (purely physical) effects, chemical and combined effects play an important role, which will be discussed in the next section.

While at the first time step shown in Fig. 8, the ignition energy dominates the kernel expansion, the relative importance of chemistry and diffusion increases at the second and third time step. Therefore, the growth of the hydrogen kernel is much faster than that of the other mixtures, even though the spark assisted flame propagation effect is much smaller. The last frame for propane illustrates the intake of unburnt gas due to the flow field induced by the discharge. As Lim et al. [15] and Ko et al. [19] pointed out, for propane/air mixtures the early kernel growth is mainly due to mass entrainment. Therefore, the flow field plays an important role for the ignition process and is a main cause of the stochastic nature observed for the ignition of propane/air mixtures. This is also true, although less distinct, for the ethene/air mixture. Since the

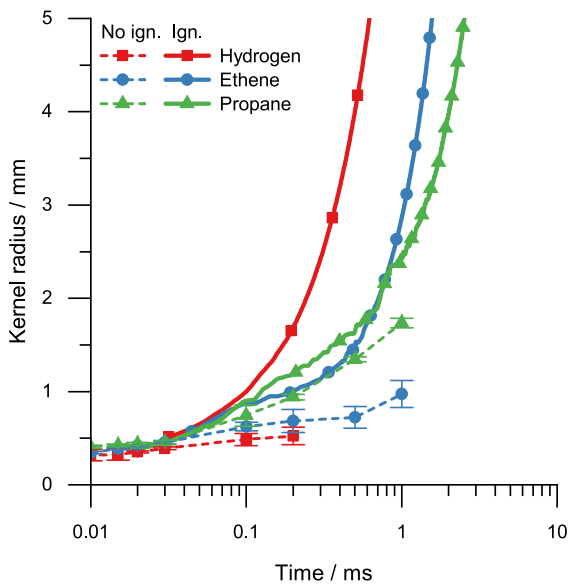


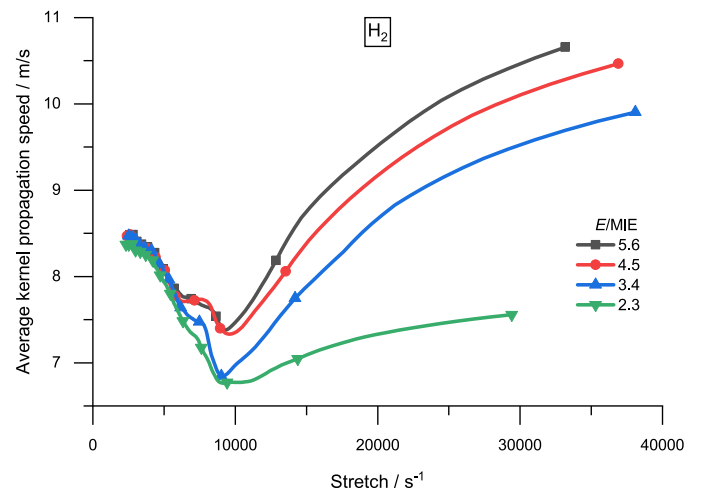
Fig. 9. Comparison of the expansion of non-igniting flame kernels (dashed lines) and igniting flame kernels (solid lines) for the three investigated mixtures. The discharge energy was $E/MIE = 1.0$ for the non-igniting kernels. For the igniting kernels, $E/MIE = 1.5$ for the ethene/air and propane/air mixture; $E/MIE = 2.3$ for the hydrogen/air mixture.

early kernel growth is not dominated by diffusion, the flow field strongly influences the flame development as is seen in Fig. 6(b).

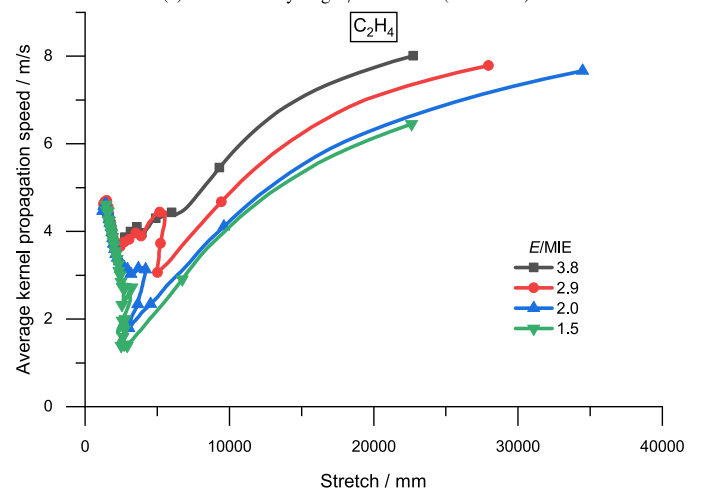
Further confirmation of the importance of the flow field on the ignition is provided by the comparison shown in Fig. 9. Here, we compare the average kernel radius for the lowest ignition energy of each mixture ($E/MIE = 2.3$ for hydrogen/air and $E/MIE = 1.5$ for ethene/air and propane/air, cf. Table 2) from Fig. 5 with the kernel expansion at $E/MIE = 1.0$. In the latter case, no ignition was observed in the experiment. The data was extracted from single-shot schlieren images from an earlier work which focused on the gas-dynamic expansion of the kernel mainly at time instances in the microsecond and sub-microsecond scales [37]. Since the mixture was not ignited in these cases, the kernel expansion is almost exclusively due to the flow induced by the discharge. It was found that the kernel expansion was split into two phases: firstly, a pressure-driven phase which lasts about $1\mu\text{s}$, and secondly, a flow-driven phase which further expands the kernel. The comparison in Fig. 9 shows that the flow accounts for roughly 70% of the kernel growth up to 1.0 ms in the propane case. Its influence is smaller but still considerably for the ethene/air mixture. In the hydrogen case, the flow effect is negligible after some 100 μs . This illustrates how the chemical reaction dominates the kernel propagation speed after a very short time. Especially for the propane/air mixture, however, the transition occurs on a longer time scale, allowing for a greater chance for perturbations and loss processes to interfere with the ignition process.

3.3. Effect of stretch and Lewis number

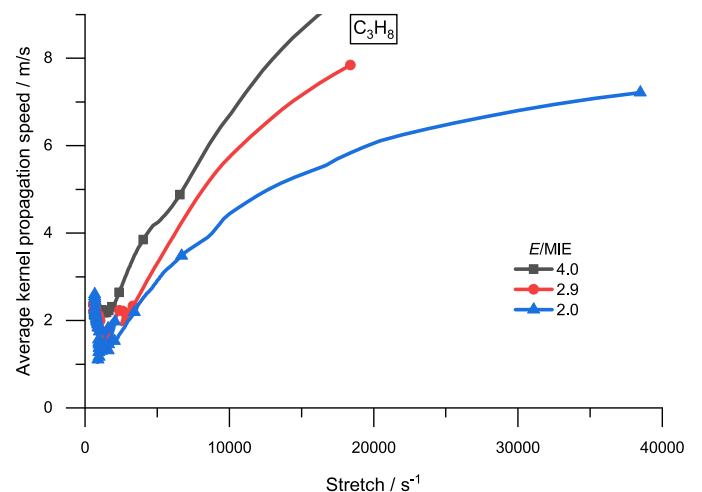
In Fig. 10, we show the average kernel propagation speed as a function of stretch K , based on the curves in Fig. 7. For spherically expanding flames, $K = 2/R_f dR_f/dt$ [45]. This plot can be used to identify different flame regimes [25]. For a short time interval, the ignition energy strongly affects the average kernel propagation speed for all mixtures. At large positive stretch, corresponding to small flame radii and early times, the flame propagation is assisted by the ignition source. Then, the average kernel propagation speed reaches a minimum value. As the ignition energy is increased, the minimum average kernel propagation speed increases. The stretch rate at which this minimum is reached depends on the gas mix-



(a) 23.3 vol. % hydrogen/air mixture ($Le = 0.56$)



(b) 8.0 vol. % ethene/air mixture ($Le = 1.11$)



(c) 5.2 vol. % propane/air mixture ($Le = 1.17$)

Fig. 10. Average kernel propagation speed over stretch for several ignition energies close to the minimum ignition energy.

ture. It is biggest for hydrogen and smallest for propane, thus, it correlates inversely with the Lewis number of the mixture.

The ethene and propane mixtures have Lewis numbers greater than unity (1.11 and 1.17, respectively, cf. Table 1). Thus, the flame propagation is impeded by positive stretch. The Lewis number of

the hydrogen mixture is 0.56, hence, positive stretch is expected to enhance the flame propagation. However, the results in Figs. 7(a) and 10(a) show that for kernel radii up to 7 mm or stretch rates smaller than 10,000/s, the average kernel propagation speed increases with decreasing stretch. This observation is contrary to the well-established fact that stretch will increase the flame propagation speed for mixtures with $Le < 1$ [25,26,46]. However, this is an asymptotic theory which assumes that the flame thickness is much smaller than the typical hydrodynamic length scale, i.e. it assumes that the hydrodynamic scale is at least a few centimeter [47]. Thus, it can only be expected to be valid at small stretch rates. For the small radii considered here ($R_f < 1$ cm), the stretch rate is not small and the flame thickness is not negligible compared to the kernel radius. Nevertheless, at energies close to the MIE, the behavior seen in Figs. 7(a) and 10(a) was predicted theoretically by He [48] when the flame kernel is still small. Only at sufficiently high ignition energy does the average kernel propagation speed become a monotonically decreasing function of the kernel radius. It is expected that the average kernel propagation speed will decrease again as the kernel continues to grow. Our data are, however, limited to kernel radii of about 8 mm since we intended to focus on the very early phase of flame propagation. The same effect was observed experimentally by Nakahara et al. [49] for lean hydrogen/air mixtures ($\varphi = 0.7$ and 0.9) as well as a rich propane/air mixture ($\varphi = 1.2$) at relatively small ignition energies, though their mixtures were diluted with additional nitrogen. They found a transitional stage at the meso-scale where the flame speed increases with increasing diameter (or decreasing stretch) while at larger radii (macro-scale) the decrease of stretch led to a decrease of flame speed. In most experimental studies, this effect for $Le < 1$ is not observed because either small kernel radii were not investigated or higher ignition energies were used. For example, Kelley et al. [46] found that for a lean hydrogen/air mixture ($\varphi = 0.30$) the flame speed decreases with increasing kernel radius. Further, they showed that increasing the ignition energy increased the flame speed up to a certain kernel radius (or stretch rate). However, the ignition energy was no smaller than 12.5 mJ [46] while the MIE at $\varphi = 0.30$ ($\nu = 8.9$ vol%) is only about 54 μ J [10] to 230 μ J [50].

Our experiments clearly illustrate how strongly the Lewis number and its interrelation with stretch influence the early phase of flame propagation and, thus, in particular, the ignition process by electrical discharges near the MIE. Chen et al. [26] investigated this interrelation numerically for several hydrogen/air, methane/air and propane/air mixtures with $Le = 0.5$ to 2.5 . A major result of their study regarded the critical flame radius which needs to be exceeded by spark assisted flame propagation. It was found that this radius increases with the Lewis number. Experimental confirmation of their theory was provided by Kelley et al. [46] for hydrogen/air and butane/air mixtures and by Kim et al. [51] for n-decane/air mixtures. Our results are in qualitative agreement with Chen et al. [26] and provide, thus, the first experimental confirmation of their findings for an ethene/air and propane/air mixture. Figure 7 shows that for the mixtures with $Le > 1$, the flame radius corresponding to the minimum of the average kernel propagation speed increases as the Lewis number increases. This value is close to the critical flame radius [46].

This finding has far-reaching implications for safety-relevant ignition processes, i.e. the ignition of burnable gas mixtures at energies close to their minimum ignition energy. In particular for mixtures with a high Lewis number, the spatial dimensions as well as the temporal duration where disturbances may interfere with the ignition process increase. Therefore, the flow field which is induced by the discharge has a stronger effect for mixtures with Lewis numbers greater than unity than for mixtures with lower Lewis numbers. Moreover, statistically distributed deviations of the

initial conditions can lead to the stochastic behavior of the ignition process, especially at a low discharge energy and a large Lewis number. These fluctuating parameters may include the temperature, pressure, mixture composition, position of the discharge location, initial flow field, discharge energy and duration, and possibly further variables. Given these points, these sub-processes are required to be modeled carefully in order to correctly predict safety-relevant ignition processes. The data provided by our experiments can potentially aid the development and validation of such numerical models. Eventually, these models could be used to assist the design and conformity assessment phases in the development process of explosion protected equipment.

A further impact of our results can be the advancement of the measurement technique to characterize the speed of spherically expanding laminar flames. Usually, the combustible gas mixture is ignited centrally by a high-energy electric discharge [25,52,53]. Presumably, the amount of imposed energy is chosen in a conservative way so that the ignition probability is virtually 100%. This choice results in an unnecessarily large energy application and, consequently, a larger radius of influence. Choosing the ignition energy carefully based on the MIE of the mixture, e.g. $E = 5$ MIE, can therefore limit unwanted effects caused by the ignition source. Thus, the experimental error can be reduced and more reliable data can be extracted.

4. Conclusions

We investigated the ignition of three burnable gas/air mixtures by electrical discharges at conditions close to the respective MIE conditions. Here, the ignition process is of a stochastic nature. High-speed schlieren imaging was applied to the early phase of flame propagation. Our experiments reveal and clarify the decline of reproducibility as the introduced energy approaches the MIE. The data provide a quantification of the stochastic flame initiation and propagation at very low energy levels. This information gives important insights into underlying physical mechanisms. Furthermore, the experiments confirm the importance of the flow field on the evolution of the ignition kernel. It was found, in agreement with previous studies, that the flow field is an important factor governing the early expansion in case the Lewis number of the mixture is relatively large. This is due to the effect of stretch on the flame speed when the Lewis number is not unity. For the hydrogen/air mixture, which has a Lewis number considerably smaller than unity, the ignition process was very repeatable and was not influenced by the flow field induced by the discharge. Further, we demonstrated the existence a mixture-dependent radius above which the kernel propagation speed is independent of the ignition source.

Consequently, numerical simulations for the prediction of safety-relevant ignition processes need to take into account at least two-dimensional effects of the electrode geometry on the flow field and where possible, the influence of stochastic fluctuations in the initial conditions in the time and space domain. Thus, improved numerical models based on detailed knowledge of the physiochemical effects governing ignition by low-energy electrical discharges could lead to extended limits for the safe operation of processes in hazardous areas. Further, they could enable economic benefits in the design and production of explosion protected devices.

Acknowledgments

The authors gratefully acknowledge the financial support by Deutsche Forschungsgemeinschaft (DFG) [grant number MA5083/1-2].

Supplementary material

Supplementary material associated with this article can be found, in the online version, at doi:[10.1016/j.combustflame.2019.09.021](https://doi.org/10.1016/j.combustflame.2019.09.021).

References

- [1] M. Kono, S. Kumagai, T. Sakai, The optimum condition for ignition of gases by composite sparks, *Symp. (Int.) Combust.* 16 (1977) 757–766, doi:[10.1016/S0082-0784\(77\)80369-X](https://doi.org/10.1016/S0082-0784(77)80369-X).
- [2] R. Maly, M. Vogel, Initiation and propagation of flame fronts in lean CH₄-air mixtures by the three modes of the ignition spark, *Symp. (Int.) Combust.* 17 (1979) 821–831, doi:[10.1016/S0082-0784\(79\)80079-X](https://doi.org/10.1016/S0082-0784(79)80079-X).
- [3] L.J. Jiang, S.S. Shy, M.T. Nguyen, S.Y. Huang, D.W. Yu, Spark ignition probability and minimum ignition energy transition of the lean iso-octane/air mixture in premixed turbulent combustion, *Combust. Flame* 187 (2018) 87–95, doi:[10.1016/j.combustflame.2017.09.006](https://doi.org/10.1016/j.combustflame.2017.09.006).
- [4] B. Lewis, G. von Elbe, *Combustion, Flames and Explosion of Gases*, second, Academic Press, New York and London, 1961.
- [5] E. Brandes, W. Möller, *Flammable Liquids and Gases: Brennbare Flüssigkeiten und Gase*, Safety Characteristic Data, 1, second, Wirtschaftsverl. NW, Bremerhaven, 2008.
- [6] S.P.M. Bane, *Spark ignition: experimental and numerical investigation with application to aviation safety*, Ph.D. thesis, California Institute of Technology, Pasadena, 2010.
- [7] R.K. Eckhoff, W. Olsen, A new method for generation of synchronized capacitive sparks of low energy. Reconsideration of previously published findings, *J. Electrostat.* 68 (1) (2010) 73–78, doi:[10.1016/j.elstat.2009.11.001](https://doi.org/10.1016/j.elstat.2009.11.001).
- [8] J. Moorhouse, A. Williams, T.E. Maddison, An investigation of the minimum ignition energies of some C₁ to C₇ hydrocarbons, *Combust. Flame* 23 (2) (1974) 203–213, doi:[10.1016/0010-2180\(74\)90058-3](https://doi.org/10.1016/0010-2180(74)90058-3).
- [9] D.R. Ballal, A.H. Lefebvre, The influence of spark discharge characteristics on minimum ignition energy in flowing gases, *Combust. Flame* 24 (0) (1975) 99–108, doi:[10.1016/0010-2180\(75\)90132-7](https://doi.org/10.1016/0010-2180(75)90132-7).
- [10] M. Hattwig, H. Steen, *Handbook of Explosion Prevention and Protection*, Wiley-VCH, Weinheim, 2004.
- [11] S.P.M. Bane, J.L. Ziegler, P.A. Boettcher, S.A. Coronel, J.E. Shepherd, Experimental investigation of spark ignition energy in kerosene, hexane, and hydrogen, *J. Loss. Prevent. Proc. Ind.* 26 (2) (2011) 290–294, doi:[10.1016/j.jlp.2011.03.007](https://doi.org/10.1016/j.jlp.2011.03.007).
- [12] S.P.M. Bane, J.E. Shepherd, E. Kwon, A.C. Day, Statistical analysis of electrostatic spark ignition of lean H₂/O₂/Ar mixtures, *Int. J. Hydrog. Energy* 36 (3) (2011) 2344–2350, doi:[10.1016/j.ijhydene.2010.05.082](https://doi.org/10.1016/j.ijhydene.2010.05.082).
- [13] R.K. Eckhoff, M. Ngo, W. Olsen, On the minimum ignition energy (MIE) for propane/air, *J. Hazard. Mater.* 175 (1–3) (2010) 293–297, doi:[10.1016/j.jhazmat.2009.09.162](https://doi.org/10.1016/j.jhazmat.2009.09.162).
- [14] A. Wähner, G. Gramse, T. Langer, M. Beyer, Determination of the minimum ignition energy on the basis of a statistical approach, *J. Loss. Prevent. Proc. Ind.* 26 (6) (2013) 1655–1660, doi:[10.1016/j.jlp.2013.06.002](https://doi.org/10.1016/j.jlp.2013.06.002).
- [15] M.T. Lim, R.W. Anderson, V.S. Arpacı, Prediction of spark kernel development in constant volume combustion, *Combust. Flame* 69 (3) (1987) 303–316, doi:[10.1016/0010-2180\(87\)90123-4](https://doi.org/10.1016/0010-2180(87)90123-4).
- [16] M. Champion, B. Deshaies, G. Joulin, K. Kinoshita, Spherical flame initiation: theory versus experiments for lean propane-air mixtures, *Combust. Flame* 65 (3) (1986) 319–337, doi:[10.1016/0010-2180\(86\)90045-3](https://doi.org/10.1016/0010-2180(86)90045-3).
- [17] M. Kono, K. Niu, T. Tsukamoto, Y. Ujiie, Mechanism of flame kernel formation produced by short duration sparks, *Symp. (Int.) Combust.* 22 (1989) 1643–1649, doi:[10.1016/S0082-0784\(89\)80176-6](https://doi.org/10.1016/S0082-0784(89)80176-6).
- [18] A. Borghese, M. Diana, V. Moccia, R. Tamai, Early growth of flames, ignited by fast sparks, *Combust. Sci. Technol.* 76 (4–6) (1991) 219–231, doi:[10.1080/00102209108951710](https://doi.org/10.1080/00102209108951710).
- [19] Y. Ko, R.W. Anderson, V.S. Arpacı, Spark ignition of propane-air mixtures near the minimum ignition energy: Part I. An experimental study, *Combust. Flame* 83 (1–2) (1991) 75–87, doi:[10.1016/0010-2180\(91\)90204-0](https://doi.org/10.1016/0010-2180(91)90204-0).
- [20] P.L. Pitt, R.M. Clements, D.R. Topham, The early phase of spark ignition, *Combust. Sci. Technol.* 78 (4–6) (1991) 289–314, doi:[10.1080/00102209108951753](https://doi.org/10.1080/00102209108951753).
- [21] K. Eisazadeh-Far, F. Parsinejad, H. Metghalchi, J.C. Keck, On flame kernel formation and propagation in premixed gases, *Combust. Flame* 157 (12) (2010) 2211–2221, doi:[10.1016/j.combustflame.2010.07.016](https://doi.org/10.1016/j.combustflame.2010.07.016).
- [22] U. Maas, J. Warnatz, Ignition processes in hydrogen-oxygen mixtures, *Combust. Flame* 74 (1) (1988) 53–69, doi:[10.1016/0010-2180\(88\)90086-7](https://doi.org/10.1016/0010-2180(88)90086-7).
- [23] M. Thiele, J. Warnatz, A. Dreizler, S. Lindenmaier, R. Schießl, U. Maas, A. Grant, P. Ewart, Spark ignited hydrogen/air mixtures: two dimensional detailed modeling and laser based diagnostics, *Combust. Flame* 128 (1–2) (2002) 74–87, doi:[10.1016/S0010-2180\(01\)00333-9](https://doi.org/10.1016/S0010-2180(01)00333-9).
- [24] R. Ono, T. Oda, Measurement of OH density and gas temperature in incipient spark-ignited hydrogen-air flame, *Combust. Flame* 152 (1–2) (2008) 69–79, doi:[10.1016/j.combustflame.2007.07.022](https://doi.org/10.1016/j.combustflame.2007.07.022).
- [25] Z. Chen, M.P. Burke, Y. Ju, Effects of Lewis number and ignition energy on the determination of laminar flame speed using propagating spherical flames, *Proc. Combust. Inst.* 32 (1) (2009) 1253–1260, doi:[10.1016/j.proci.2008.05.060](https://doi.org/10.1016/j.proci.2008.05.060).
- [26] Z. Chen, M.P. Burke, Y. Ju, On the critical flame radius and minimum ignition energy for spherical flame initiation, *Proc. Combust. Inst.* 33 (1) (2011) 1219–1226, doi:[10.1016/j.proci.2010.05.005](https://doi.org/10.1016/j.proci.2010.05.005).
- [27] M. Zhou, G. Li, Z. Zhang, J. Liang, L. Tian, Effect of ignition energy on the initial propagation of ethanol/air laminar premixed flames: an experimental study, *Energy Fuels* 31 (9) (2017) 10023–10031, doi:[10.1021/acs.energyfuels.7b00965](https://doi.org/10.1021/acs.energyfuels.7b00965).
- [28] M. Kono, S. Kumagai, T. Sakai, Ignition of gases by two successive sparks with reference to frequency effect of capacitance sparks, *Combust. Flame* 27 (1976) 85–98, doi:[10.1016/0010-2180\(76\)90008-0](https://doi.org/10.1016/0010-2180(76)90008-0).
- [29] S.P.M. Bane, J.L. Ziegler, J.E. Shepherd, Investigation of the effect of electrode geometry on spark ignition, *Combust. Flame* 162 (2) (2015) 462–469, doi:[10.1016/j.combustflame.2014.07.017](https://doi.org/10.1016/j.combustflame.2014.07.017).
- [30] B. Singh, L.K. Rajendran, M. Giarra, P.P. Vlachos, S.P.M. Bane, Measurement of the flow field induced by a spark plasma using particle image velocimetry, *Exp. Fluids* 59 (12) (2018) 034018, doi:[10.1007/s00348-018-2632-y](https://doi.org/10.1007/s00348-018-2632-y).
- [31] T. Redeker, Classification of flammable gases and vapours by the flame-proof safe gap and the incendivity of electrical sparks, Report PTB-W-18, Physikalisch-Technische Bundesanstalt, 1981, ISSN: 0341-6739.
- [32] J. Munro, Are the IEC requirements for overpressure testing of flameproof equipment appropriate? 2016 Petroleum and Chemical Industry Conference Europe (PCICEurope), IEEE, Piscataway, NJ (2016), pp. 1–10, doi:[10.1109/PCICEurope.2016.7850286](https://doi.org/10.1109/PCICEurope.2016.7850286).
- [33] T. Langer, G. Gramse, D. Mückel, U. von Pidoll, M. Beyer, MIE experiments and simultaneous measurement of the transferred charge – a verification of the ignition threshold limits, *J. Electrostat.* 70 (2012) 97–104.
- [34] R. Addabbo, J.K. Bechtold, M. Matalon, Wrinkling of spherically expanding flames, *Proc. Combust. Inst.* 29 (2) (2002) 1527–1535, doi:[10.1016/S1540-7489\(02\)80187-0](https://doi.org/10.1016/S1540-7489(02)80187-0).
- [35] D.G. Goodwin, H.K. Moffat, R.L. Speth, Cantera: An Object-oriented Software Toolkit for Chemical Kinetics, Thermodynamics, and Transport Processes, 2017, doi:[10.5281/zenodo.170284](https://doi.org/10.5281/zenodo.170284).
- [36] G.P. Smith, D.M. Golden, M. Frenklach, N.W. Moriarty, B. Eiteneer, M. Goldenberg, C.T. Bowman, R.K. Hanson, S. Song, W.C. Gardiner Jr., V.V. Lissianski, Z. Qin, GRI-MECH 3.0, 1999, <http://combustion.berkeley.edu/gri-mech/version30/text30.html>.
- [37] S. Essmann, D. Markus, U. Maas, Investigation of the spark channel of electrical discharges near the minimum ignition energy, *Plasma Phys. Technol.* 3 (3) (2016) 116–121.
- [38] S. Essmann, S. Spörhase, H. Grosshans, D. Markus, Precise triggering of electrical discharges by ultraviolet laser radiation for the investigation of ignition processes, *J. Electrostat.* 91 (2018) 34–40, doi:[10.1016/j.elstat.2017.12.003](https://doi.org/10.1016/j.elstat.2017.12.003).
- [39] G.S. Settles, *Schlieren and Shadowgraph Techniques: Visualizing Phenomena in Transparent Media*, Engineering Online Library, Springer, Berlin, 2001.
- [40] M. Thiele, J. Warnatz, U. Maas, Geometrical study of spark ignition in two dimensions, *Combust. Theor. Model.* 4 (4) (2000) 413–434, doi:[10.1088/1364-7830/4/4/303](https://doi.org/10.1088/1364-7830/4/4/303).
- [41] B. Sforzo, A. Lambert, J. Kim, J. Jagoda, S. Menon, J. Seitzman, Post discharge evolution of a spark igniter kernel, *Combust. Flame* 162 (1) (2015) 181–190, doi:[10.1016/j.combustflame.2014.07.024](https://doi.org/10.1016/j.combustflame.2014.07.024).
- [42] D. Bradley, F.K.-K. Lung, Spark ignition and the early stages of turbulent flame propagation, *Combust. Flame* 69 (1) (1987) 71–93, doi:[10.1016/0010-2180\(87\)90022-8](https://doi.org/10.1016/0010-2180(87)90022-8).
- [43] J. Warnatz, U. Maas, R.W. Dibble, *Combustion: Physical and Chemical Fundamentals, Modeling and Simulation, Experiments, Pollutant Formation*, fourth, Springer, Berlin, 2006.
- [44] K. Ishii, T. Tsukamoto, Y. Ujiie, M. Kono, Analysis of ignition mechanism of combustible mixtures by composite sparks, *Combust. Flame* 91 (2) (1992) 153–164, doi:[10.1016/0010-2180\(92\)90097-9](https://doi.org/10.1016/0010-2180(92)90097-9).
- [45] M. Matalon, On flame stretch, *Combust. Sci. Technol.* 31 (3–4) (1983) 169–181, doi:[10.1080/00102208308923638](https://doi.org/10.1080/00102208308923638).
- [46] A.P. Kelley, G. Jomaas, C.K. Law, Critical radius for sustained propagation of spark-ignited spherical flames, *Combust. Flame* 156 (5) (2009) 1006–1013, doi:[10.1016/j.combustflame.2008.12.005](https://doi.org/10.1016/j.combustflame.2008.12.005).
- [47] M. Matalon, C. Cui, J.K. Bechtold, Hydrodynamic theory of premixed flames: effects of stoichiometry, variable transport coefficients and arbitrary reaction orders, *J. Fluid Mech.* 487 (2003) 179–210, doi:[10.1017/S0022112003004683](https://doi.org/10.1017/S0022112003004683).
- [48] L. He, Critical conditions for spherical flame initiation in mixtures with high Lewis numbers, *Combust. Theor. Model.* 4 (2) (2000) 159–172, doi:[10.1088/1364-7830/4/2/305](https://doi.org/10.1088/1364-7830/4/2/305).
- [49] M. Nakahara, F. Abe, K. Tokunaga, A. Ishihara, Fundamental burning velocities of meso-scale propagating spherical flames with H₂, CH₄ and C₃H₈ mixtures, *Proc. Combust. Inst.* 34 (2013) 703–710, doi:[10.1016/j.proci.2012.08.007](https://doi.org/10.1016/j.proci.2012.08.007).
- [50] B. Lewis, G. von Elbe, *Combustion, Flames and Explosions of Gases*, third, Academic Press, Orlando, 1987.
- [51] H.H. Kim, S.H. Won, J. Santner, Z. Chen, Y. Ju, Measurements of the critical initiation radius and unsteady propagation of n-decane/air premixed flames, *Proc. Combust. Inst.* 34 (1) (2013) 929–936, doi:[10.1016/j.proci.2012.07.035](https://doi.org/10.1016/j.proci.2012.07.035).
- [52] A.G. Giannakopoulos, A. Gatzoulis, C.E. Frouzakis, M. Matalon, G.K. Tomboulides, Consistent definitions of “Flame Displacement Speed” and “Markstein Length” for premixed flame propagation, *Combust. Flame* 162 (4) (2015) 1249–1264, doi:[10.1016/j.combustflame.2014.10.015](https://doi.org/10.1016/j.combustflame.2014.10.015).
- [53] A.N. Lipatnikov, S.S. Shy, W.-y. Li, et al., Experimental assessment of various methods of determination of laminar flame speed in experiments with expanding spherical flames with positive Markstein lengths, *Combust. Flame* 162 (7) (2015) 2840–2854, doi:[10.1016/j.combustflame.2015.04.003](https://doi.org/10.1016/j.combustflame.2015.04.003).